Thermochimica Acta 493 (2009) 80–84

Contents lists available at ScienceDirect

Thermochimica Acta

journal homepage: www.elsevier.com/locate/tca

Interrupted thermal desorption of TiH_2

Ch. Borchers[a,*], T.I. Khomenko[b], A.V. Leonov[c], O.S. Morozova[b]

[a] Institute of Material Physics, University of Göttingen, Friedrich-Hund-Platz 1, 37077 Göttingen, Germany
[b] Semenov Institute of Chemical Physics RAS, 4 Kosygin St, 119991 Moscow, Russia
[c] Moscow State University, Department of Chemistry, Leninskie Gory, 119899 Moscow, Russia

ARTICLE INFO

Article history:
Received 12 November 2008
Received in revised form 30 March 2009
Accepted 15 April 2009
Available online 23 April 2009

Keywords:
Thermal desorption spectroscopy
X-ray diffraction
Phase stability
Titanium monohydride

ABSTRACT

Structural changes of commercial TiH_2 were studied using interrupted temperature desorption spectroscopy and X-ray diffraction techniques to understand the mechanism of its degradation under non-equilibrium conditions. Rapid cooling on different stages of temperature-programmed heating allowed to study the intermediate phase compositions that evolve upon cooling from the high-temperature phase βTi(H). The phase transformation sequence is described as a number of consecutive reactions corresponding to the observed desorption peaks. Phases δTiH_{2-x}, γTiH, and the solid solution αTi(H) were found to be intermediates in the $\varepsilon TiH_2 \rightarrow \alpha Ti$ transformation when the latter is interrupted. Additional evidence for the thermodynamic stability of γTiH is given.

1. Introduction

The development in metal-hydride technology requires a detailed study of hydrogen interaction with metals and alloys [1]. In order to improve hydrogen absorption–desorption kinetics, the charging and discharging procedures (i.e. hydride formation and decomposition) have to be carried out under non-equilibrium heating conditions. Temperature-programmed sorption/desorption may be successfully applied for this purpose.

The technique of thermal desorption spectroscopy (TDS) is widely used in various modifications as an effective method for a quantitative description of gas–solid surface interactions [2–6]. It is especially useful to test the key parameters of adsorption and catalytic processes: properties and energy distribution of active sites [7–11]. In this technique, the samples are heated, and the hydrogen evolution from the sample is monitored simultaneously. Han et al. [12] were among the first who used thermal desorption spectra to study hydrogen desorption kinetics from MgH_2 and to determine the rate-controlling step. Nowadays, this technique is commonly used to demonstrate the effect of preparation or treatment conditions on H_2 desorption kinetics for different metal-hydrides [13–20].

The decomposition of metal-hydride under non-equilibrium conditions is a multi-stage process, the mechanism of which is poorly studied. However, this knowledge is essential to attain the most important commercial requirement: to significantly accelerate hydrogen sorption and desorption at lower temperatures.

For two reasons Ti-hydride is a perfect model compound for such investigations: (i) it is widely used as a component of hydrogen storage materials, and especially as foaming agent to produce metal foams [21–23]; (ii) its interaction with hydrogen is studied in detail [24–29].

In this work, we apply step-by-step heating in thermal desorption regime interrupted by a fast sample cooling to study mechanisms of non-equilibrium decomposition of commercial TiH_2 by testing intermediate phase compositions. By doing this, the different phases can be attributed to the different desorption peaks. Furthermore, the thermodynamic stability of the titanium monohydride γTiH is confirmed once again by testing long-term stability of the detected phases. This has been disputed in literature for some time [30–33], but is now consensus [26 and references therein].

2. Experimental

Commercial TiH_2 powder (Aldrich, 99% pure, 325 mesh, $S = 0.32\ m^2/g$) with an actual composition $TiH_{1.92}$ was used. The H_2 desorption, i.e. TiH_2 decomposition, was studied by thermal desorption spectroscopy (TDS). TDS measurements were carried out at a heating rate of 10.5–11.2 K/min from 293 to 1030 K under flow conditions at a flow rate of 100 ml/min using pure Argon. A quartz flow-reactor was charged with 0.1 g of TiH_2 powder mixed with ~70 wt.% of quartz powder in order to minimize the temperature difference between the sample and surroundings caused by the heat of reaction and to prevent powder caking. The sam-

* Corresponding author. Tel.: +49 551 395584; fax: +49 551 395012.
E-mail address: chris@ump.gwdg.de (Ch. Borchers).

0040-6031/$ – see front matter © 2009 Elsevier B.V. All rights reserved.
doi:10.1016/j.tca.2009.04.011

Table 1
TDS parameters for TiH_2 calculated on base of Lorentzian fitting of TDS spectrum.

Peak	H_2 evolution [$\times 10^{-4}$ mol]	T_{max} [K]	E_a [kJ/mol]
1	3.9×10^{-3} (19.5 at.%)	743	219.5 ± 6.5
2	1.23×10^{-2} (61.6 at.%)	817	229.7 ± 7.2
3	3.8×10^{-3} (18.9 at.%)	920	216.1 ± 7.3

ple was heated up to the chosen temperature, these are namely 785, 838, 925, and 1030 K, and then rapidly cooled to room temperature by transferring the reactor from the heater to ice water. Each TDS run was carried out with fresh TiH_2 powder. Hydrogen emission was monitored continuously by a gas chromatograph. The hydrogen portion being desorbed was calculated from the integral intensity of the TDS spectrum. The effective activation energy (E_a) for different stages of TiH_2 decomposition was estimated from linear Arrhenius plots constructed assuming that the H_2 evolution rate is proportional to the hydrogen concentration in the sample. XRD patterns were recorded after each TDS experiment using a Dron-3 diffractometer with Cu Kα radiation. The phase composition of the respective powders was determined on base of JCPDS files provided by the International Center for Diffraction Data. Quantitative X-ray phase analysis was performed applying a fitting procedure, where experimental spectra were approximated with a linear combination of the theoretical spectra of phases and of the background using optimized values of lattice parameters and parameters of broadening of the diffraction maxima of phases. The respective hydrogen content of the samples was calculated on base of material balance. Samples heated to 756 and 838 K were reheated until total desorption of hydrogen to test the independence of the desorption peaks and to be able to relate the phase changes to the desorption peaks. In order to test the stability of the phases, a sample heated to 838 K was studied by X-ray diffraction and studied a second time after ageing for 48 h at room temperature.

3. Results

Fig. 1 shows a thermal desorption spectrum of the total TiH_2 decomposition. It consists of one rather narrow main peak (T_{max} = 817 K) and one low- and one high-temperature shoulder ($T_{max} \approx$ 743 and 920 K, respectively). The process parameters calculated on base of Lorentzian fitting of the TDS curve are summarized in Table 1. The Lorentzian fits of each peak are added in Fig. 1.

Hydrogen desorption observed during TDS is accompanied by structural transformations of the TiH_2 up to total decomposition.

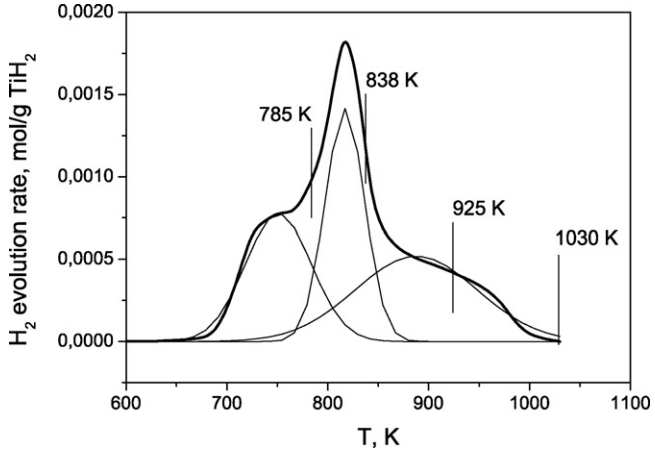

Fig. 1. TDS spectrum of Ti-hydride: vertical lines point to temperatures of heating interruption.

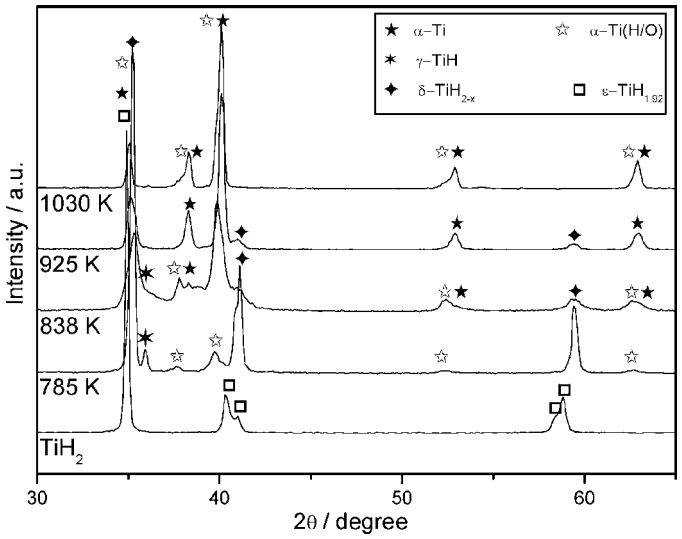

Fig. 2. Structural evolution of TiH_2 after TDS interrupted at 785, 838, 925 and 1030 K as compared to the structure of original TiH_2.

To establish a correspondence between the TD-spectrum and structural evolution during decomposition the phase composition of powder was determined by XRD after different steps of TDS, which are marked in Fig. 1. Table 2 summarizes corresponding TDS and XRD data. Fig. 2 shows the XRD spectra of the original TiH_2 compared to the spectra recorded after TDS was interrupted at 785, 838, 925, and 1030 K, which correspond to the end of the first TDS peak, the end of the main peak, the falling slope of the high-temperature peak, and to the total TDS, respectively.

The original Ti-hydride containing 1.92 H/Ti was identified as tetragonal ε phase, JCPDS 25-983, space group *I*4/*mmm* with lattice constants a = 0.447 nm, c = 0.441 nm. After TDS was interrupted at 785 K, the sample still contains 1.33 H/Ti. There are two Ti-hydride phases: about 70 wt.% of cubic δTiH_{2-x} (a = 0.440 nm), about 15 wt.% of a new phase, which is most probably the orthorhombic phase γTiH (JCPDS 44-1217) besides about 15 wt.% of the solid solution αTi(H). The composition of αTi(H) solid solution is calculated as Ti-8.5 at.% H from the hydrogen induced increase of the αTi unit cell volume, 0.28 nm^3/H [34]. After TDS is interrupted at 838 K, the sample contains 0.61 H/Ti. A remarkable elevated and jittery intensity was observed in the interval 2θ = 33.5–42.5°, in which only two peaks could be identified unambiguously. Due to this, the quantitative phase analysis was troublesome. The following phases were detected: δTiH_{2-x} (a = 0.440 nm; less than 30 wt.%), the same γTiH, and two hexagonal phases: αTi (a = 0.295 nm, c = 0.468 nm) and αTi-6.3 at.% H solid solution (a = 0.297 nm, c = 0.476 nm). The phase composition of the TDS product after heating up to 925 K consists of about 15 wt.% of δTiH_{2-x} (a = 0.440), and two hexagonal phases: about 70 wt.% of αTi (a = 0.295 nm, c = 0.468 nm) and about 15 wt.% of αTi-3 at.% H solid solution (a = 0.296 nm, c = 0.473 nm). According to material balance, the total system contains 0.18 H/Ti. The TiH_2 decomposition was completely finished at 1030 K. However, besides the αTi phase (a = 0.295 nm, c = 0.469 nm), some amount of hexagonal phase with a = 0.296 nm, c = 0.474 nm was detected. Since virtually the total H_2 has evolved this leads one to assume oxygen dissolution in Ti lattice because of extremely high Ti to oxygen affinity at T > 1000 K.

Fig. 3 shows a comparison of TPD spectra of (1) the fresh TiH_2 powder and (2) TiH_2 powder heated up to 756 K in (a), cooled rapidly and heated again in TPD regime; and a comparison of TPD spectra of (1) the fresh TiH_2 powder and (2) TiH_2 powder heated up to 838 K, cooled rapidly and heated again in TPD regime in (b). It can clearly be seen that the left shoulder of the original spectrum

Table 2
XRD parameters.

T [K]	Residual H [H/Ti]	Phase composition (JCPDS–Nr.)	Portion [wt.%]	Lattice parameters [nm]
293	1.92	$\varepsilon TiH_{1.92}$ (25–983)	[100]	$a = 0.447$; $c = 0.441$
785	1.33	δTiH_{2-x} (07–370) γTiH (44–1217) αTi(H)	[70] [15] [15]	$a = 0.440$ $a = 0.297$; $c = 0.479$
838	0.61	δTiH_{2-x} (07–370) γTiH (44–1217) αTi(H) αTi	[<30]	$a = 0.440$ $a = 0.297$; $c = 0.476$ $a = 0.295$; $c = 0.468$
925	0.18	δTiH_{2-x} (07–370) αTi(H) αTi	[15] [15] [70]	$a = 0.440$ $a = 0.296$; $c = 0.473$ $a = 0.295$; $c = 0.468$
1030	0.04	αTi(O) αTi	[25] [75]	$a = 0.296$; $c = 0.474$ $a = 0.295$; $c = 0.469$

is the imprint of an independent peak. The same holds for the right shoulder of the TD-spectrum.

To test the stability of the detected phases, a sample cooled from 838 K was aged at room temperature for 48 h and subsequently X-rayed again. An increase in αTi, γTiH, and a decrease in αTi(H) content were observed. After 48 h, the phase composition remained stable.

4. Discussion

Fig. 5 shows the phase diagram of the Ti–H system [25]. The Initial position, $\varepsilon TiH_{1.92}$, is marked with a star in the lower right corner. The upward arrows denote the respective temperature/hydrogen content positions from which the quenches are performed. Already at 785 K/1.33 H/Ti the sample is within the βTi(H)–δTiH_{2-x} two-phase region. At 838 K/0.61 H/Ti, the sample is quenched from pure βTi(H). According to this phase diagram, there is no stable hydride in the two-phase region αTi(H)–δTiH_{2-x}. In a recent re-assessment performed by Manchester and San-Martin, however, γTiH is included as a stable phase at H/Ti ratio of 1.0 in the temperature range below 441 K [26].

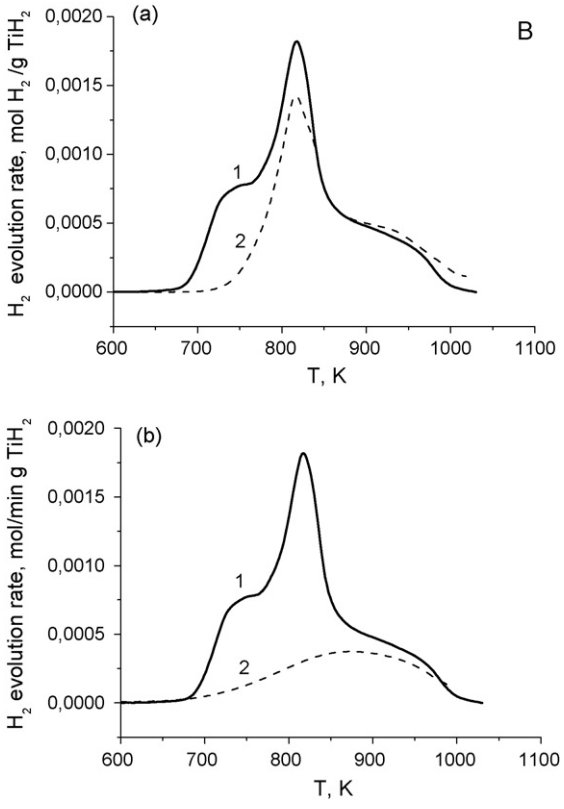

Fig. 3. (a) TiH_2 powder heated up to 756 K, cooled rapidly and heated again in TDS regime; comparison of TD-spectra of (1) the fresh TiH_2 powder and (2) TiH_2 powder heated up to 838 K, cooled rapidly and heated again in TDS regime. (b) As in (a), but heated up to 838 K.

The phase γTiH is face-centered orthorhombic, where the H atoms occupy half of the tetrahedral sites in an ordered fashion. While in early works, γTiH is supposed to be metastable [30,31], recent first principle calculations performed by Xu and Van der Ven [32] demonstrate that γTiH is a Ti-hydride stable relative to fcc-Ti at low temperatures below about 450 K and "almost stable" relative to hcp Ti. This means that the formation energy of γTiH is just above that of αTi(H) + δTiH_{2-x}. This finding is confirmed by experimental results from Bashkin and co-workers [33], who find that γTiH is stable at low temperatures below 473 K. Since the peritectic transformation αTi(H) + $\delta TiH_{2-x} \rightarrow \gamma$TiH is hampered because of slow diffusion and elastic stress [34], this phase is often not at all observed in cooling experiments [e.g. 35]. The results presented in this work confirm that γTiH is a stable phase at low temperatures: after room temperature ageing of the sample quenched from 838 K the amount of γTiH has augmented, corroborating the results published by Manchester and San-Martin [26 and references therein].

The phase γTiH can mainly be identified by the peak at 36°, corresponding to a lattice plane distance $d = 0.25$ nm. The other peaks are either of very low intensity or they lie beneath peaks corresponding to δTiH_{2-x} or αTi(H), which is also the reason why we do not give lattice parameters for this phase. Of course the identification of a phase with only one peak that can unambiguously be attributed to this phase is difficult. There are several other Ti-hydrides listed in the JCPDS files with a prominent peak near 36°, but all of these except γTiH are stated to be metastable or are not applicable either for thermodynamic reasons or because there should be other prominent peaks not found in our spectra. Because of the growth of this peak upon room temperature ageing pointing to thermal stability, we believe to indeed have found γTiH. As can be seen in Fig. 2, the amount of γTiH found is only appreciable in the samples cooled from 785 and 838 K, but not in the sample cooled from 925 K. In the case of the sample cooled from 785 K, see Fig. 5, a large proportion of the sample passes through the δTiH_{2-x} single phase region and leaves it at a temperature below the peritectic temperature of γTiH. If our considerations are correct, this proportion will directly transform into γTiH + δTiH_{2-x}, where γTiH is the minority component, corresponding to the 70 wt.% of δTiH_{2-x} and 15% of γTiH found in this sample besides 15% of αTi(H). For the sample cooled from 838 K, the greatest part of the sample passes

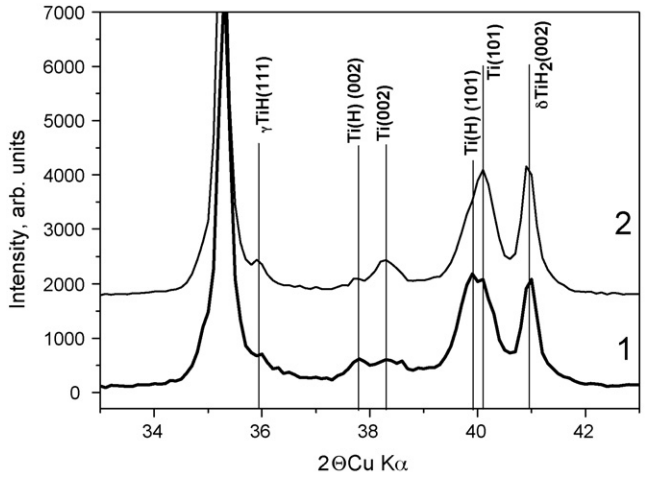

Fig. 4. Fragment of XRD patterns of powder heated to 838 K: (1) recorded immediately after the TPD run and (2) after 48 h.

the eutectoid point 571 K/42.5 at.% (0.74 H/Ti, data from [26]). Here, the temperature difference between βTi(H) and the peritectic temperature of γTiH is only 130 K, which makes it probable enough that some proportion of the material transforms into γTiH, which can in our case roughly be estimated as 10% from the experimental data, and which is given as 10% at most in literature [33]. In case of the sample cooled from 925 K, only about 30% of the sample passes through the eutectoid point as can be estimated by the lever rule. If 10% of this material transforms into γTiH, this cannot be detected by XRD keeping in mind that there is peak broadening due to small powder particle size.

As can be seen in Fig. 4, the phase composition immediately after rapid cooling is not completely in thermal equilibrium. It includes the metastable hexagonal αTi(H) solid solution, which decomposes into αTi and γTiH. In terms of this result and on base of XRD data the phase transformation sequence for TiH_2 decomposition under non-equilibrium conditions can be schematized as follows:

$$\varepsilon TiH_{1.92} \rightarrow \delta TiH_{2-x} \rightarrow \beta Ti(H) \rightarrow \{\delta TiH_{2-x} + \gamma TiH+\}\alpha Ti(H) \rightarrow \alpha Ti,$$

where βTi(H) as a high-temperature phase is not detected by XRD, but its existence is postulated from the phase diagram, see Fig. 5. $\{\delta TiH_{2-x} + \gamma TiH+\}$ is put into brackets because this transformation only takes place when the thermal desorption process is interrupted and the sample cooled, but not when it is continued.

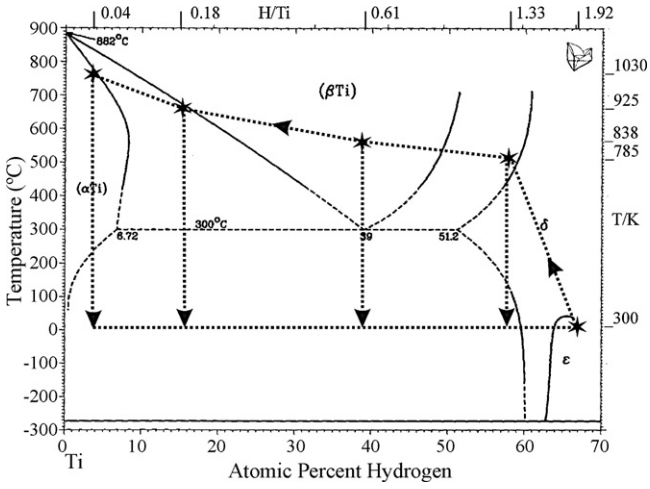

Fig. 5. Ti–H phase diagram [25]. Stars (experimental points) mark heating interruption temperature and corresponding hydrogen content in the sample.

The total decomposition process may be formally divided into three parts corresponding to the three peaks of the TD-spectrum. The first peak with T_{max} = 743 K may be attributed to the $\varepsilon TiH_2 \rightarrow \delta TiH_{2-x}$ transition caused by H_2 loss. Fig. 3a shows that this shoulder completely disappeared from the TDS spectrum (curve 1), after the sample was heated in thermal desorption regime up to 785 K, then rapidly cooled and heated again (curve 2). The second peak with T_{max} = 817 K mainly reflects the transformation $\delta TiH_{2-x} \rightarrow \beta Ti(H)$, and the transformation $\beta Ti(H) \rightarrow \alpha Ti(H) \rightarrow \alpha Ti$ seems to be responsible for the high-temperature shoulder which is formally the high-temperature Lorentzian peak, see Fig. 3b.

Thermal desorption of TiH_2 has been studied in numerous other groups; see, e.g. [21–23,36–38]. The results are not completely consistent. Kennedy and Lopez, Lehmhus and Rausch as well as Fernández et al. found two-peak spectra [21,22,36], Yang et al. found four peaks [23], while von Zeppelin et al. and Bhosle et al. recorded one-peak spectra [37,38], both with small pre-peaks. These different results cannot be due to the heating rate, as was shown by Fernández et al.: heating rates between 5 and 20 K/min differ only in peak positions, but not the peak structure [36]. However, Lehmhus and Rausch showed impressively that the decomposition spectra are quite sensitive to the atmosphere during decomposition as well as to the atmosphere the powder was exposed to before desorption study [22]. This, if not poorly resolved spectra, might be the reason for the observed differences. Yang et al. give values for activation energies E_a that can be compared to the values found in this work, see Table 1. They found four peaks (given in pairs of values T_{max}[K]/E_a[kJ/mol]): 740/125, 852/184, 940/677, and 980/200. Our results yielded 743/220, 817/230, and 920/216. Obviously, correspondence is not given for the high-temperature range, most probably for one of the reasons given above.

To summarize, the results presented demonstrate that: (i) the TDS peaks are independent and point to a well-defined reaction each and (ii) γTiH is indeed a thermodynamically stable phase. The latter result has been disputed in the past but is consensus since the year 2000 at latest.

5. Conclusions

Interrupted TDS technique was successfully applied to investigate the mechanism of TiH_2 decomposition under non-equilibrium conditions. The phases δTiH_{2-x}, γTiH, and the solid solution αTi(H) were found to be intermediates in $\varepsilon TiH_2 \rightarrow \alpha Ti$ transformation, when the sample is cooled to room temperature at different intermediate stages.

The phase proportions observed upon rapid cooling were found to be metastable. The stabilization of phase composition went through an increase in γTiH and αTi, i.e. Ti-hydride and Ti metal, and a decrease in Ti(H) solid solution.

Acknowledgements

The authors are thankful for RFBR, project no. 07-03-00610 and INTAS, project no. 05-1000005-7672, which partly supported this work.

References

[1] K.M. MacKay, Hydrogen Compounds of the Metallic Elements, Spon, London, 1965.
[2] J.W. Niemantsverdriet, Spectroscopy in Catalysis. An Introduction, VCH, Weinheim, NY, Basel, Cambridge, Tokyo, 1993 (P.2 Temperature-programmed Techniques).
[3] S.A.J. Lombardo, A.T. Bell, Surf. Sci. Reports 13 (1991) 3–72.
[4] M. Mavrikakis, J.W. Schwank, J.L. Gland, Phys. Chem. 100 (1996) 11389–11395.
[5] M.U. Kislyuk, Kinetika i Kataliz 43 (2002) 645 (in Russian).
[6] H. Froitzheim, P. Schenk, G. Wedler, J. Vac. Sci. Technol. A 11 (1993) 345–353.

[7] Z. Chang, W.H. Tang, Surf. Sci. 601 (2007) 2005–2011.
[8] Y. Yokoi, H. Uchida, Catal. Today 42 (1998) 167–174.
[9] H. Zou, X. Dong, W. Lin, Appl. Surf. Sci. 253 (2006) 2893–2898.
[10] J.L. Ayastuy, M.P. Gonzalez-Marcos, J.R. Gonzalez-Velasco, M.A. Gutierrez-Ortiz, Appl. Catal. B., Environ. 70 (2007) 532–541.
[11] R. Wojcieszak, S. Monteverdi, J. Ghanbaja, M.M. Bettahar, J. Colloid Interface Sci. 317 (2008) 166–174.
[12] J.S. Han, M. Pezat, J.-Y. Lee, J. Less-Comm. Metals 130 (1987) 395–402.
[13] A. Zaluska, L. Zaluski, J.O. Ström-Olsen, Appl. Phys. A 72 (2001) 157–165.
[14] T. Ogawa, K. Yokoyama, K. Asaoka, J. Sakai, J. Alloys Compds. 396 (2005) 269–274.
[15] T. Zecho, A. Güttler, J. Küppers, Carbon 42 (2004) 609–617.
[16] V.D. Dobrovol'skii, O.G. Radchenko, Y.M. Solonin, V.B. Muratov, I.A. Morozov, Metallofiz. Noveishie Tekhnol. 28 (2006) 303–311 (in Russian).
[17] F.J. Castro, G. Meyer, J. Alloys Compds. 330–332 (2002) 59–63.
[18] E.Z. Kurmaev, O.S. Morozova, T.I. Khomenko, Ch. Borchers, S.N. Nemnonov, Y. Harada, T. Tokushima, H. Osawa, T. Takeuchi, S. Shin, J. Alloys Compds. 395 (2005) 240–246.
[19] Ch. Borchers, A.V. Leonov, T.I. Khomenko, O.S. Morozova, J. Mater. Sci. 39 (2004) 5259–5262.
[20] Ch. Borchers, O.S. Morozova, T.I. Khomenko, A.V. Leonov, A.V. Postnikov, E.Z. Kurmaev, A. Moewes, A. Pundt, J. Phys. Chem. C 112 (2008) 5869–5976.
[21] A.R. Kennedy, V.H. Lopez, Mater. Sci. Eng. A357 (2003) 258–263.
[22] D. Lehmhus, G. Rausch, Adv. Eng. Mater. 6 (2004) 313–330.
[23] D.H. Yang, B.Y. Hur, D.P. He, S.R. Yang, Mater. Sci. Eng. A 445–446 (2007) 415–426.
[24] A.D. McQuillan, Proc. Roy. Soc. A204 (1950) 309–322.
[25] A. San-Martin, F.D. Manchester, Bull. Alloy Phase Diag. 8 (1987) 30–42.
[26] F.D. Manchester, A. San-Martin, in: F.D. Manchester (Ed.), Phase Diagrams of Binary Hydrogen Alloys, ASM International, USA, 2000, pp. 238–258.
[27] F.D. Manchester, J. Chem. Phys. 115 (2001) 8557–8562.
[28] A.L. Shilov, Z.V. Dobrokhotova, L.N. Padurez, Zh. Neorg. Khimii 45 (2000) 1279–1282 (in Russian).
[29] A.L. Ivanovsky, V.A. Gubanov, E.Z. Kurmaev, J. Phys. Chem. Solids 46 (1985) 823–829.
[30] H. Numakura, M. Koiwa, Acta Metall. 32 (1799) 1984.
[31] H. Numakura, M. Koiwa, H. Asano, F. Izumi, Acta Metall. 36 (1988) 2267.
[32] Q. Xu, A. Van der Ven, Phys. Rev. B 76 (2007) 064207.
[33] I.O. Bashkin, V.Y. Malyshev, E.G. Ponyatovsky, Z. Phys. Chem. 179 (1993) 119.
[34] Y. Fukai, The Metal-Hydrogen System. Basic Bulk Properties, Springer-Verlag, Berlin, 1993.
[35] G.F. Kobzenko, A.P. Kobzenko, M.V. Chubenko, V.V. Pet'kov, A.V. Polenur, Int. J. Hydrogen Energy 20 (1995) 383–386.
[36] J.F. Fernández, F. Cuevas, C. Sánchez, J. Alloys Compds. 298 (2000) 244–253.
[37] F. von Zeppelin, M. Haluška, M. Hirscher, Thermochim. Acta 404 (2003) 251–258.
[38] V. Bhosle, E.G. Baburaj, M. Miranova, K. Salama, Mater. Sci. Eng. A356 (2003) 190–199.